Appl Biochem Biotechnol (2010) 162:805–822
DOI 10.1007/s12010-010-8912-5

Mercury(II) Biosorption Using *Lessonia* sp. Kelp

Mariana Reategui · Holger Maldonado · Martha Ly · Eric Guibal

Received: 13 July 2009 / Accepted: 10 January 2010 /
Published online: 14 February 2010

Abstract *Lessonia nigrescens* and *Lessonia trabeculata* kelps have been tested for the sorption of mercury from aqueous solutions. A pretreatment (using $CaCl_2$) allowed stabilizing the biomass that was very efficient for removing Hg(II) at pH6–7. Sorption isotherms were described by the Langmuir equation with sorption capacities close to 240–270 mg Hg g^{-1} at pH6. The temperature had a negligible effect on the distribution of the metal at equilibrium. The presence of chloride anions had a more marked limiting impact than sulfate and nitrate anions. The uptake kinetics were modeled using the pseudo-second-order equation that fitted better experimental data than the pseudo-first-order equation. The particle size hardly influenced sorption isotherms and uptake kinetics, indicating that sorption occurs in the whole mass of the biosorbent and that intraparticle mass transfer resistance was not the limiting rate. Varying the sorbent dosage and the initial metal concentration influenced the equilibrium, but the kinetic parameters were not drastically modified. Metal can be eluted with hydrochloric acid, citric acid, or acidic KI solutions.

Keywords Mercury(II) · *Lessonia* · Kelp · Isotherms · Kinetics · Pseudo-second-order equation · Desorption

Introduction

The mining and metallurgical activities produce large flows of contaminated water containing high concentrations of metal ions. The regulations concerning water discharge

Electronic supplementary material The online version of this article (doi:10.1007/s12010-010-8912-5) contains supplementary material, which is available to authorized users.

M. Reategui · H. Maldonado · M. Ly
Departamento Académico de Química, Universidad Peruana Cayetano Heredia, Av. Honorio Delgado, 430 Urbanización Ingeniería, Lima 31, Peru

M. Reategui · E. Guibal (✉)
Laboratoire Génie de l'Environnement Industriel, Ecole des Mines d'Alès, 6 avenue de Clavières, 30319 Alès cedex, France
e-mail: Eric.Guibal@ema.fr

to the environment are becoming more and more drastic, and there is a need for alternative processes for the treatment of these industrial effluents [1]. Indeed, precipitation processes are commonly used. However, they are, in most cases, inappropriate for reaching levels of decontamination required by the regulations. Sophisticated precipitants are required for reaching target levels [2]. Membrane processes such as polymer-enhanced ultrafiltration [3] or reverse osmosis can be applied, but the process is expensive for large-scale applications. Solvent extraction processes are generally used for the recovery of metal ions from highly concentrated solutions [4, 5]. Adsorption, ion exchange, and chelating resins are suitable for the treatment of medium range of concentration [6–8]. However, these processes are generally too expensive when applied at large scale. Biosorption is a process that was widely investigated for the last decades [9–11]. It consists in using materials of biological origin for the sorption of metal ions from dilute solutions. A number of biomass have been tested for metal recovery, including fungi [9–12], bacteria [13], yeasts, and algae [14–18] but also biopolymers such as chitin and chitosan (derived from fungal biomass or crustacean shells) [6] and alginate (derived from algal biomass) [19]. These processes use the reactive groups present at the surface of the microorganisms for the binding of metal ions as it occurs with ion exchange and chelating resins. However, these materials are issued from renewable resources making the process more compatible with a sustainable growth. Additionally, at the end of the life cycle, the material is generally eliminated more environmentally friendly than synthetic resins, which, for example, can produce hazardous materials when incinerated [20].

Mercury ions are among the most hazardous metal ions that can be discharged to the environment, due to their accumulative effect in the food chain and to the health impact it may cause. The Minamata's event is one of the most emblematic examples of the impact of mercury intake: The accumulation of mercury in the food chain caused the contamination of fish resource and the further poisoning of local populations by fish food.

In a previous work, five algae and kelps (*Lessonia nigrescens* Bory, *Prionitis decipiens*, *Grateloupia doryphora*, *Lessonia trabeculata*, and *Macrocystis integrifolia*) collected on the coast of Peru were tested for mercury sorption [21]. These preliminary results showed that *Lessonia* sp. sorbents were the most efficient. This work focuses on the extensive investigation of sorption properties of *L. nigrescens* and *L. trabeculata* for Hg(II) biosorption. The first part of the work deals with the influence of pH on sorption properties. The sorption isotherms have been determined at selected pH and varying temperature. The uptake kinetics are compared for varying experimental conditions: sorbent dosage (SD, grams per liter), metal concentration (C_0, milligram per liter), particle size (PS, micrometer). The influence of environmental parameters (presence of salts, presence of metals…) is also considered in relation with metal speciation. Desorption was also considered using acidic solutions and potassium iodide solutions.

Material and Methods

Materials

The biomass was collected on the Peruvian coast (in the Tacna area for *L. trabeculata* and in the Bahia de Paracas, Pisco, for *L. nigrescens* Bory). They have been identified by the Phytology Section of the Botanical Department at the Biological Sciences Faculty of the Universidad Mayor de San Marcos (Peru). After being washed with demineralized water,

the biomass was cut and dried (in an oven at 50 °C for 24 h). Dried biomass was finally crushed and sieved according the following size fractions:

$$\mathrm{PS}: 0-80\ \mu\mathrm{m}\ /\ 80-125\ \mu\mathrm{m}\ /\ 125-250\ \mu\mathrm{m}\ /\ 250-500\ \mu\mathrm{m}$$

Some organic material can be leached from biomass during the sorption process [22]. This organic material may cause precipitation or complexation of metal ions, which, in turn, may affect metal sorption properties on solid biomass. To prevent this leaching, the biomass was pretreated using calcium chloride solutions [23]. Forty grams of dry biomass were agitated for 24 h in 20 mL of 0.2 M $CaCl_2$ (the pH being controlled to 5 with NaOH and HNO_3 solutions). Finally, the treated biomass was rinsed four times with demineralized water before being dried in an oven at 50 °C for 24 h.

Most of the salts were supplied by Fluka, except $ZnCl_2$ (obtained from Riedel-de-Haen). All metal salts were used under the form of chloride salts.

Experimental Procedures

Sorption isotherms (and experiments at equilibrium) were performed by contact of the sorbent with the solution (with a sorbent dosage of 0.2 $\mathrm{g\,L^{-1}}$) at fixed concentration (C_0, in the range 10–160 mg metal per liter) and fixed pH, under agitation using a reciprocal shaker at the agitation speed of 400 movement/min. Samples were collected and filtered after 3 days of contact. The pH was not adjusted during sorption step, but it was systematically measured at equilibrium and compared with the initial pH. Residual metal concentration (C_{eq}, milligram per liter) was determined using an inductively coupled plasma atomic emission spectrometer (ICP-AES) JY 2000. The impact of competitor ions (and ionic strength) was determined using a similar procedure: The salt was directly added to the initial Hg(II) solution. Sorption capacity q (milligram of Hg per gram) was calculated using the mass balance equation $q = \left(C_0 - C_{eq}\right)V/m$, where V is the volume of solution (liter) and m is the amount of sorbent (gram; V/m is the reciprocal of the sorbent dosage).

Uptake kinetics were obtained by contact of 1 L of solution (at fixed pH and metal concentration) with a given amount of biosorbent. Since all these parameters (metal concentration, particle size, sorbent dosage, etc.…) have been varied, the experimental conditions will be systematically reported in the caption of the figures. Samples were collected, filtered, and analyzed for residual metal concentration to obtain the kinetic profile ($C(t)/C_0$ versus time, t). In most cases, experiments were performed at room temperature (20±1 °C); when the temperature was varied (to 40 °C), the experiments were performed in a thermostatic box. The experimental conditions have been selected appropriately for making possible the detection of intraparticle diffusion resistance. With an excess of sorbent relative to metal content, the sorption may be only located on the external layers of the biosorbent, and the intraparticle diffusion cannot express its limiting effect.

The analysis of speciation diagram of mercury in solution shows that with an excess of chloride ions (concentration eight times higher than the concentration of mercury), the metal does not precipitate at pH 7. In this study, mercury was supplied under the form of the dichloride salt. Additionally, the pH was controlled using both NaOH and HCl. It results that chloride ions were in excess compared to mercury ions making possible the formation of chloro-species that increase mercury solubility. Blank tests showed that the metal loss with a 200 mg Hg $\mathrm{L^{-1}}$ solution at pH 7.1 did not exceed 3%. On the basis of a 2:1 molar ratio between chloride and mercury (salt stoichiometric ratio, without external addition), mercury begins to precipitate at pH 6.2, at the concentration of 200 mg Hg $\mathrm{L^{-1}}$, and at pH 7

for a concentration of 50 mg Hg L^{-1}. The interaction of the biomass with the solution may result at the surface of the sorbent to variations of the pH limited to the near environment of the particles. This variation may cause localized microprecipitation ("local" pH different to the pH of the solution), which, in turn, overestimates the sorption by combining microprecipitation and sorption. For this reason, the data obtained at pH 7 should be taken with caution. However, the blank experiments showed that this impact is limited.

Preliminary tests of desorption were operated by contact of a given amount of sorbent saturated with metal ions with a series of eluting agents: mineral acids, complexing agents, including acid solutions (0.1 M HCl, 0.1 M H_2SO_4, 0.1 M HNO_3, 0.05 and 0.5 M citric acid, and 0.25 M KI in 0.1 M HCl), alkaline, or neutral solutions (0.1 M $NaHCO_3$, 0.1 M $(NH_4)_2SO_4$, and 1 M NaCl). The objective of this study was to identify the best eluent and to evaluate the reversibility of the sorption and not really to estimate the concentration effect. For this reason, the experimental conditions such as amount of sorbent (i.e., 50 mg) and volume of solution (i.e., 80 mL) for both the sorption and the desorption steps were identical, and the efficiency of desorption was measured comparing the decrease of mercury concentration (for the sorption) and the concentration of the metal in the eluate (for desorption). At the end of the sorption step, the biomass was recovered by filtration and rinsed to remove absorbed water containing mercury prior to be mixed with the eluent.

Scanning electron microscopy (SEM) and SEM-EDAX (SEM coupled with energy dispersive X-ray analysis) were performed using an Environmental Scanning Electron Microscopy (ESEM) Quanta FEG 200, equipped with an OXFORD Inca 350 Energy Dispersive X-ray microanalysis system. The system can be used to acquire qualitative or semi-quantitative spot analyses, elemental maps and line scans. This ESEM allows samples to be analyzed at pressures and humidity which approach normal laboratory conditions and avoids experimental artifact. More specifically, this is possible to analyze the samples at much higher pressure than with conventional SEM.

Modeling of Sorption Isotherms and Uptake Kinetics

The distribution of the metal at the equilibrium between the two phases was modeled using the Langmuir equation, which is represented by the equation:

$$q = \frac{q_m b C_{eq}}{1 + b C_{eq}} \tag{1}$$

where q and q_m (mg g^{-1}) show the sorption capacity in equilibrium with residual concentration (C_{eq}, milligram per liter) and at saturation of the monolayer, respectively; b (liter per milligram) is the affinity constant of the sorbent for given metal ions.

The kinetics have been modeled using three conventional models: (a) the pseudo-first-order rate equation (PFORE; the so-called Lagergren equation), (b) the pseudo-second-order rate equation (PSORE) [24], and (c) the simplified approach of intraparticle diffusion (the so-called Weber and Morris model).

PFORE [25]:

$$\frac{dq(t)}{dt} = k_1 \left(q_{eq} - q(t)\right) \tag{2}$$

and after integration:

$$\ln\left(1 - \frac{q(t)}{q_{eq}}\right) = -k_1 t \tag{3}$$

where q_{eq} (milligram per gram) is the sorption capacity at equilibrium (experimental value) and k_1 (per minute) is the pseudo-first-order rate constant.

PSORE [24]:

$$\frac{dq(t)}{dt} = k_2\left(q_{eq} - q(t)\right)^2 \tag{4}$$

and after integration:

$$q(t) = \frac{q_{eq}^2 k_2 t}{1 + q_{eq} k_2 t} \tag{5}$$

After linearization:

$$\frac{t}{q(t)} = \frac{1}{k_2 q_{eq}^2} + \frac{1}{q_{eq}} t \tag{6}$$

where q_{eq} (milligram per gram) is the sorption capacity at equilibrium (calculated value from experimental data) and k_2 (grams per milligram per minute) is the pseudo-second-order rate constant.

Simplified intraparticle diffusion resistance equation [25]:

$$q(t) = k_I t^{0.5} + I \tag{7}$$

where k_I (milligram per gram $h^{-0.5}$) is the intraparticle diffusion rate and I is the ordinate intercept representative of the possible contribution of film diffusion resistance.

The three models were tested for each set of experimental data; the best fit was systematically obtained with the pseudo-second-order rate equation (see Fig. A1 of the Electronic Supplementary Material).

Results and Discussion

Sorbent Characterization—SEM-EDAX Analysis

SEM-EDAX analysis was used for the characterization of sorbent surface before and after Hg(II) sorption. Figure 1a (magnification ×100) shows the secondary electron microphotographs of a series of particles of treated *L. nigrescens*: The aspect of the particles was not homogeneous. The presence of mercury on the sorbent is materialized by clearer zones. The SEM-EDAX analysis confirms that the variation in the color density is representative of significant differences. Two zones (referenced as Spectre 1 and Spectre 3) of different color density have been analyzed in detail, and the intensity of the mercury peak was about two times greater for the clear zone (i.e., Spectre 1) than for the dark zone (i.e., Spectre 3). The comparison of the spectra (Fig. 1b) shows that the sample with lower mercury content is characterized by a higher Ca content. The heterogeneity in mercury sorption is probably due to heterogeneities in the sorbent. Indeed, the composition of the cell wall depends on the growth stage: The proportion of alginate depends on the depth at which the kelps are grown, seasonal variations, and even the physical part of the kelp. Mata et al. [26] did not observe such heterogeneities using *Fucus vesiculosus* for Cd(II), Pb(II), and Cu(II) sorption.

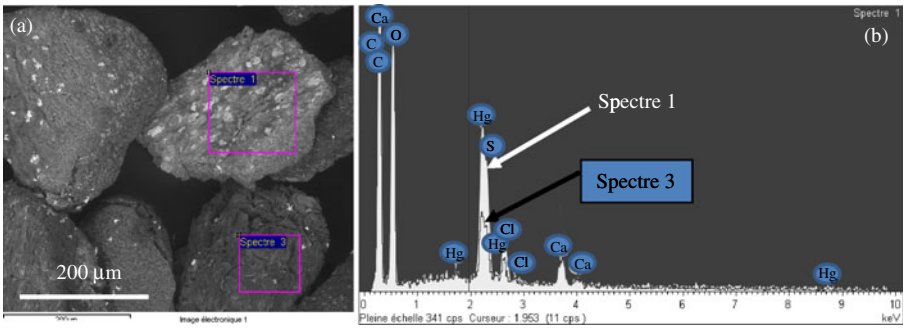

Fig. 1 Scanning electron microphotograph (secondary electrons) (**a**) and electron disperse spectrum for zones 1 and 3 (**b**) for sample of treated *L. nigrescens*

The sorption of mercury did not significantly change the structure of the biomass surface (Fig. 2, higher magnification ×1,000); the only difference between the raw material and the material loaded with Hg(II) results from the change in the color of the surface as pointed out above. Similar results were obtained with *L. trabeculata* (not shown).

Influence of pH

The pH is a parameter that usually affects sorption performance through different mechanisms: (a) impact on surface properties of the sorbent (protonation or deprotonation, competition of protons with cations) and (b) speciation of the metal. Prior to investigating sorption performance, the impact of pH was evaluated for raw biomass and treated biomass of *L. nigrescens* and *L. trabeculata* (Fig. 3). Initial values of pH were 2.0, 3.0, 4.0, 5.0, 6.0, and 7.0. This figure plots the sorption capacity versus the equilibrium pH, under selected experimental conditions. During the sorption, the pH varied in most cases: At pH2, the variation is negligible; at pH3 to 4 (around the pK_a values of carboxylic groups present on the biomass), the pH tended to increase by 0.1 to 0.3 pH unit; above pH4, the pH tended to decrease by 0.5 to 0.8 pH unit. This figure shows that the pretreatment of the biomass did

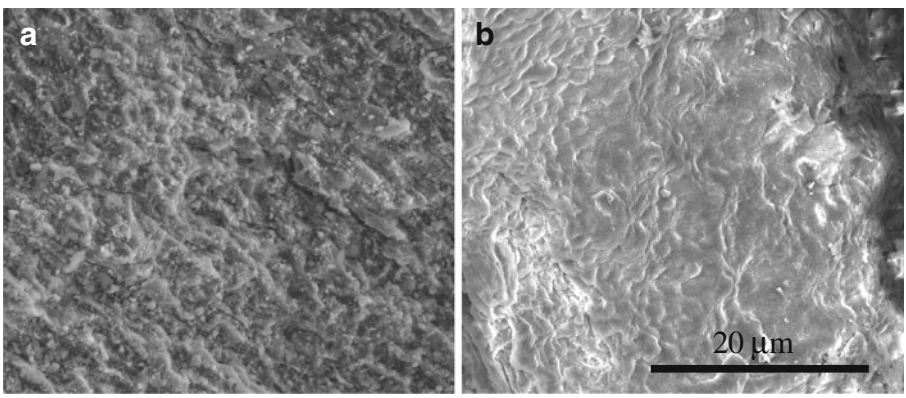

Fig. 2 Scanning electron microphotograph (secondary electrons) of *L. nigrescens* before (**a**) and after (**b**) Hg (II) sorption

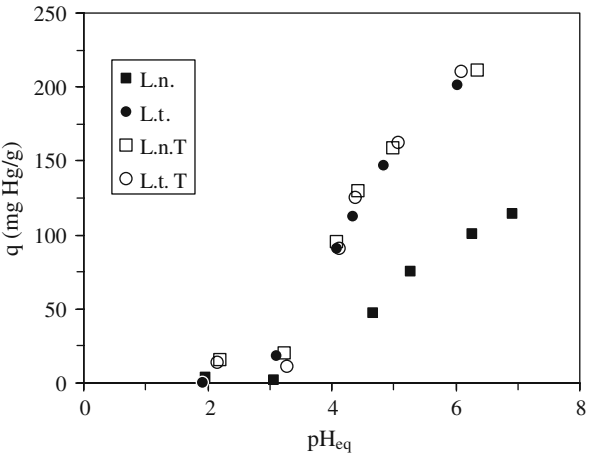

Fig. 3 Influence of pH on Hg(II) sorption using *L. nigrescens* (*L.n.*) and *L. trabeculata* (*L.t.*; as raw material and after treatment, *T*; PS 0–80 μm; C_0 50 mg L^{-1}; SD 0.2 gL^{-1}; agitation speed, *v* 200 rpm; contact time, t_∞ 3 days; temperature, *T* 20 °C)

not change the sorption properties of *L. trabeculata*, while for *L. nigrescens*, the sorption was considerably improved (by up to 80–100%, depending on initial pH) [23].

Increasing the pH reduces the competition of protons against mercury species for interacting with alginate (i.e., carboxylic groups) and other polysaccharides present on the cell wall. This contributes to increasing sorption capacity (above pH3). Alginate is a heteropolysaccharide formed of α-L-guluronic acid residues (G) and β-D-mannuronic acid (M) residues linked by 1,4 bonds. These residues may be distributed homogeneously $(\text{-M-G-})_n$ or blockwise $(\text{-M-})_n$, $(\text{-G-})_n$. These acid residues have dissociation constants close to 3.38 and to 3.65 for mannuronic acid and guluronic acid units, respectively [27]. Above pH4, the carboxylic groups become more and more deprotonated allowing a more efficient binding of mercury.

The calculation of mercury speciation (using $HgCl_2$ salt for the preparation of the solutions) shows that nonionic species predominate in the solution. The mechanism of sorption can consist in the displacement of metal speciation (to formation of mercury cations) due to the progressive sorption of residual Hg^{2+} ions (direct interaction of cations with carboxylic groups and to a lesser extent of sulfonic groups of fucoidan, present in lower quantities) or the exchange of one Cl^- with carboxylic groups.

Malik et al. used a series of kelps (including *Lessonia flavicans*) for the sorption of Cu (II), Ni(II), and Cd(II) [28]. They also observed a strong increase in the sorption capacity with increasing pH. On the contrary for As(V), Hansen et al. showed that sorption capacity decreased with pH using *L. nigrescens* [29].

It is also interesting to observe that the pH-edge curves for *L. nigrescens* and *L. trabeculata* after pretreatment superimposed. The taxonomic differences did not influence sorption properties regarding pH impact.

Sorption Isotherms

The sorption isotherms have been determined for treated biomass of *L. nigrescens* and *L. trabeculata* at pH5–7 (Fig. 4). Though some dispersion can be observed in the data

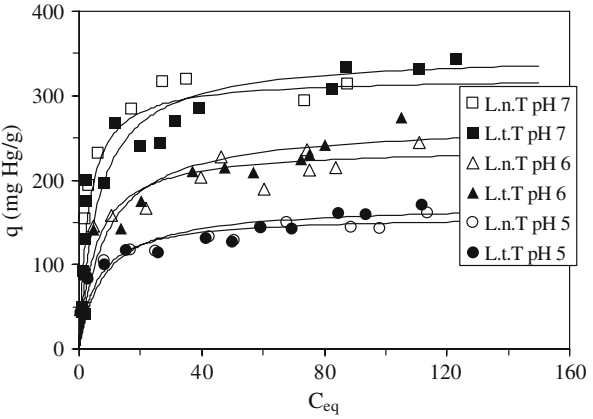

Fig. 4 Influence of initial pH on Hg(II) sorption isotherms using treated biomass of *L. nigrescens* and *L. trabeculata* (PS 125–250 μm; t_∞ 3 days; T 20 °C; v 200 rpm)

(probably due to the heterogeneity of the sorbent as shown in MEB characterization), the trends followed by the sorption capacity versus the equilibrium concentration correspond to the conventional shape of favorable isotherms. As expected from Fig. 3, increasing the pH of the solution causes the increase of sorption capacity. This experiment confirms on a wide range of metal concentration and, up to biomass saturation, the positive effect of the deprotonation of carboxylic groups. Additionally when the pH increases, the speciation of mercury changes with formation of $Hg(OH)_2$ and Hg(OH)Cl species, instead of $HgCl_2$. Though negligible precipitation was observed for the experiments on the whole range of pH investigated in this section, the variation of pH during metal sorption may cause partial precipitation; the data obtained at initial pH7 should thus be considered carefully (being slightly overestimated).

The isotherms are characterized by the appearance of a plateau at high residual concentration of Hg(II). The Langmuir equation will better fit experimental data than the Freundlich (which is characterized by a power-type equation).

Table 1 shows the values of the parameters of the Langmuir equation; they were used for plotting the modeled curves (continuous lines) on Fig. 4.

As expected from Fig. 3, the differences between *L. nigrescens* and *L. trabeculata* were not very marked. This is confirmed by the values of the constants of the Langmuir model: except at pH7 (the affinity coefficient was doubled for *L. nigrescens* compared to *L.*

Table 1 Modeling of sorption isotherms using the Langmuir equation for Hg(II) recovery using *L. nigrescens* and *L. trabeculata* (after pretreatment)—effect of initial pH and temperature.

		L. nigrescens (treated)			*L. trabeculata* (treated)		
pH	T (°C)	q_m (mg g^{-1})	b (L mg^{-1})	R^2	q_m (mg g^{-1})	b (L mg^{-1})	R^2
5	20	157.3	0.18	0.990	170.7	0.13	0.980
6	20	238.5	0.19	0.982	266.8	0.12	0.979
7	20	321.2	0.34	0.994	349.2	0.16	0.992
6	40	260.6	0.18	0.989	256.8	0.17	0.990

trabeculata), the other values were of the same order of magnitude. The maximum sorption capacity (sorption capacity at saturation of the monolayer) was systematically higher for *L. trabeculata* (by 8% to 12%) to the values reached with *L. nigrescens*. The maximum sorption capacity was close to 164 mg g^{-1} (i.e., 0.82 mmol g^{-1}) at pH5, 253 mg g^{-1} (i.e., 1.26 mmol g^{-1}) at pH6, and 335 mg g^{-1} (i.e., 1.67 mmol g^{-1}) at pH7. These values are of the same order of magnitude than the values cited by Malik et al. [28] for the sorption of Cu (II) (i.e., 1.3 mmol g^{-1}), Cd(II) (i.e., 0.9 mmol g^{-1}), and Ni(II) (i.e., 0.8 mmol g^{-1}) using *L. flavicans* at pH4. Hansen et al. [29] used *L. nigrescens* for the sorption of As(V) at different pH: They found maximum sorption capacities that decreased with the pH from 45 mg g^{-1} at pH2.5 to 28 mg g^{-1} at pH6.5. Ghodbane and Hamdaoui [30] obtained much lower sorption capacities at using eucalyptus bark (around 33 mg g^{-1}, i.e., 0.16 mmol g^{-1}). Zeroual et al. [10] used *Ulva latuca* (a seaweed biomass) for mercury sorption. They found sorption capacities ranging between 27 and 149 mg g^{-1} for pH increasing from 2.5 to 7. The sorption capacities found in the present work are also greater than the values obtained by Kaçar et al. [31] for Hg(II) and Cd(II) sorption using *Penicillium chrysosporum* (live or heat-inactivated biomass immobilized in alginate capsules): 84 mg g^{-1} for living biomass and up to 172 mg g^{-1} for heat-inactivated biomass (and only 32 mg g^{-1} for alginate material used as the encapsulating material). With *Chlamydomonas reinhardtii* immobilized in alginate beads, Bayramoğlu et al. [32] showed a maximum sorption capacity close to 110 mg g^{-1} for Hg(II) at pH6. Lloyd-Jones et al. [33] compared Hg(II) sorption isotherms at pH4 and 6 for activated carbon, a biosorbent (*Azolla filiculoides*), and two chelating ion exchange resins (Purolite S-920 and Rohm and Haas GT-73). When using activated carbon and the biosorbent, they find relatively low sorption capacities (about 0.1–0.5 mmol g^{-1}), while with the synthetic resins, under comparable conditions, the maximum sorption capacities reached up to 3–3.5 mmol g^{-1} (though the affinity was relatively weak, based on the initial slope of the isotherm curve).

A complementary experiment was carried out at higher temperature (i.e., T=40 °C) in order to evaluate the impact of temperature on the affinity of the sorbent for mercury. Actually, the differences were not marked: The difference did not exceed 10–15% for maximum sorption capacity and even lower for the affinity coefficient.

The sorption process takes place at the surface of the sorbent. However, due to the intrinsic porosity of the material, internal sorption sites may be available. It is important to check if these internal reactive groups are really accessible. The comparison of sorption capacities for sorbents of different sizes may be useful for addressing this question. Figure 5 compares for *L. nigrescens* and *L. trabeculata* the sorption capacities obtained at pH6 and 7 for different particle sizes. The variations observed in the sorption capacities are not significant (at least for *L. trabeculata*), and it is possible to conclude that the internal sites can be accessed.

Uptake Kinetics

Influence of Particle Size

The size of biosorbent particles hardly affected the sorption kinetics (Fig. 6). A slight decrease is observed when increasing the size of the particles. Indeed, increasing the size of the particles may cause a longer time for the solute to diffuse to the internal sites (intraparticle diffusion control), and it also contributes to decreasing the external available surface (film diffusion control). The differences are more marked for *L. trabeculata* than for *L. nigrescens*.

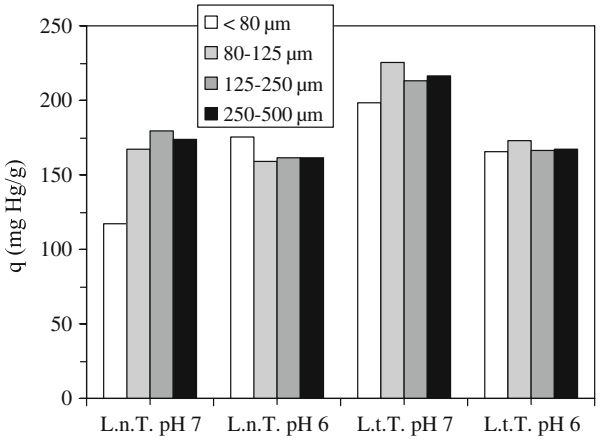

Fig. 5 Influence of particle size on Hg(II) sorption using treated biomass of *L. nigrescens* and *L. trabeculata* at different initial pH (C_0 50 mg L^{-1}; SD 0.2 gL^{-1}; T 20°C; v 200 rpm)

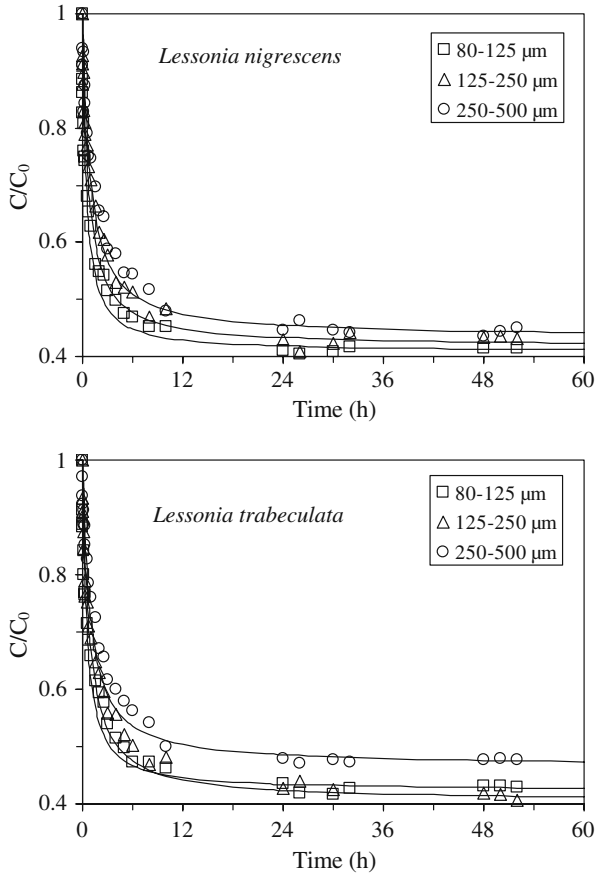

Fig. 6 Influence of particle size on Hg(II) uptake kinetics using treated biomass of *L. nigrescens* and *L. trabeculata* (C_0 50 mg L^{-1}; pH_i6; SD 0.2 gL^{-1}; T 20°C, v 400 rpm)

Table 2 reports the parameters of the pseudo-second-order rate equation. The calculated value of the sorption capacity at equilibrium correlated well with experimental values. The differences were generally lower than 3% and never exceeded 6%. The equilibrium sorption capacity was slightly decreased (by less than 10–15%). Additionally, the rate parameter (i.e., k_2) tended to decrease with increasing the size of the particles. However, this variation was essentially detectable for particle size lower than 125 μm (above, the differences were not marked enough). Though of the same order of magnitude, the parameters for *L. nigrescens* were slightly greater than those obtained with *L. trabeculata*. The weak effect of particle size on kinetic profiles and model constants confirm that the intraparticle diffusion is not the rate-limiting step. The continuous lines on the figure show the modeling of experimental data using the parameters listed in Table 2. The modeled curve fitted experimental data well. This is a confirmation that the pseudo-second-order rate equation is appropriate for modeling the kinetic profiles. Pavasant et al. [34] observed a decrease of the time required for reaching equilibrium with ground biomass (*Caulerpa lentillifera*). The sorption mechanism was quite fast (about 30 min); however, the biomass was in very large excess, i.e., 16.7 gL^{-1} of sorbent for a metal concentration of 10 mg L^{-1}. These experimental conditions are not representative of a potential application at large scale.

Influence of Sorbent Dosage

Increasing sorbent dosage improves metal recovery, though at the expense of a decrease in the sorption capacity. Figure 7 shows that experimental data are well fitted by the pseudo-second-order rate equation. The two biosorbents follow the same trend for the rate parameter k_2 that linearly increased with increasing sorbent dosage (Table 2). Increasing the amount of sorbent allows a greater number of reactive groups (and a

Table 2 Modeling of uptake kinetics using the pseudo-second-order rate equation for Hg(II) sorption using *L. nigrescens* and *L. trabeculata* at pH6.

Biomass	PS (μm)	C_0 (mg L^{-1})	SD (g L^{-1})	q_{exp} (mg g^{-1})	q_{eq} (mg g^{-1})	$k_2 \times 10^4$ (g $mg^{-1} min^{-1}$)	R^2
L.n.	80–125	50	0.2	142.3	144.1	2.64	1.000
L.n.	125–250	50	0.2	140.3	142.6	1.71	0.999
L.n.	250–500	50	0.2	130.6	134.5	1.34	0.999
L.t.	80–125	50	0.2	134.2	135.8	2.41	0.999
L.t.	125–250	50	0.2	139.4	139.8	1.48	0.994
L.t.	250–500	50	0.2	120.7	123.2	1.48	0.999
L.n.	125–250	50	0.4	96.4	97.4	3.40	1.000
L.n.	125–250	50	0.2	140.3	142.6	1.71	0.999
L.n.	125–250	50	0.1	186.2	189.8	0.73	0.997
L.t.	125–250	50	0.4	90.4	90.5	3.90	1.000
L.t.	125–250	50	0.2	139.4	139.8	1.48	0.999
L.t.	125–250	50	0.1	194.3	200.2	0.89	0.999
L.n.	125–250	15	0.2	68.1	69.3	2.89	1.000
L.n.	125–250	80	0.2	165.2	165.6	1.50	0.999
L.t.	125–250	15	0.2	68.9	70.0	3.59	1.000
L.t.	125–250	80	0.2	152.8	161.7	1.94	0.999

L.n. L. nigrescens, *L.t. L. trabeculata*

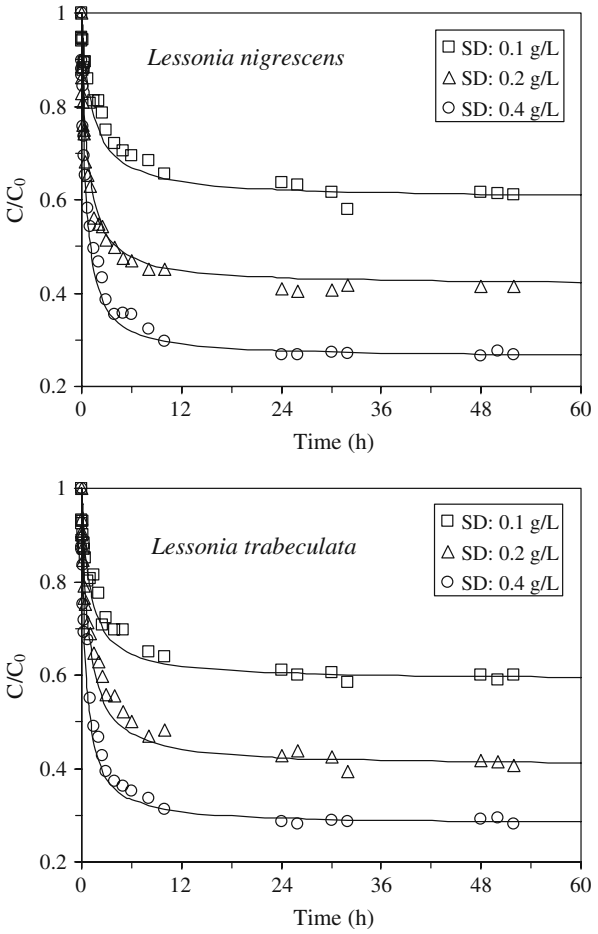

Fig. 7 Influence of sorbent dosage on Hg(II) uptake kinetics using treated biomass of *L. nigrescens* and *L. trabeculata* (C_0 50 mg L^{-1}; pH_i6; PS 125–250 μm; *T* 20 °C, *v* 400 rpm)

greater surface) to be available. The comparison of the values of model parameters shows that they changed by less than 10–15% for the two biosorbents (under similar experimental conditions). There was again a good correlation between experimental values for the sorption capacity at equilibrium and those obtained during the modeling of kinetic profiles. Even with a sorbent dosage of 0.4 gL^{-1}, mercury was not completely removed from the solution (at the initial concentration of 50 mg Hg L^{-1}). A greater mass ratio (biosorbent/Hg) should be used. The equilibrium time (approximated by the time required for reaching 95% of total sorption) appeared independent of sorbent dosage and tended to be reached within 24 h.

Influence of Metal Concentration

Figure 8 shows for both *L. nigrescens* and *L. trabeculata* the kinetic profiles when the concentration of mercury varied between 15 and 80 mg L^{-1}. As expected, the increase

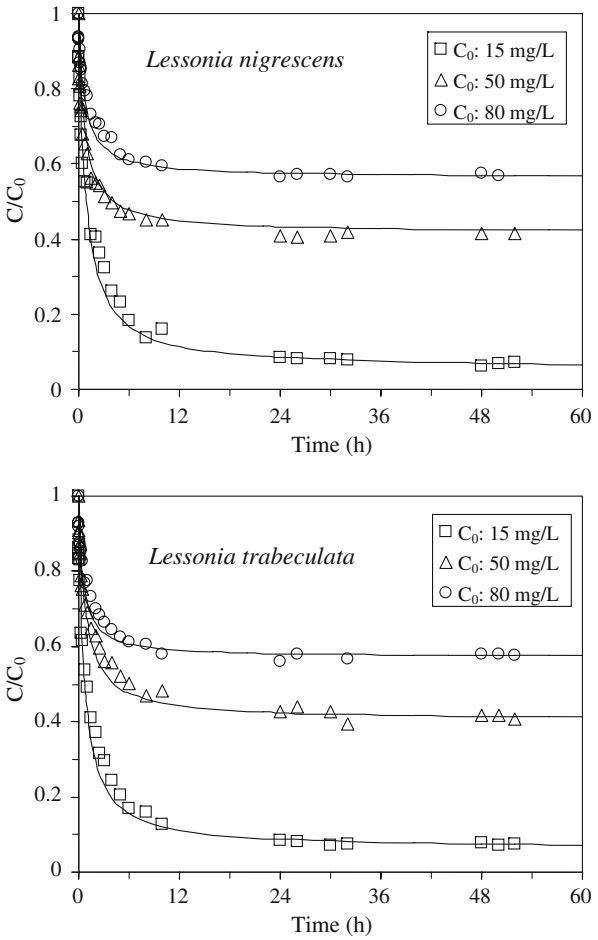

Fig. 8 Influence of metal concentration on Hg(II) uptake kinetics using treated biomass of *L. nigrescens* and *L. trabeculata* (SD 0.2 gL^{-1}; pH_i6; PS 125–250 μm; *T* 20 °C, *v* 400 rpm)

of initial concentration allowed increasing the sorption capacity at equilibrium (the experimental values and the calculated values remained in good agreement), following the sorption isotherm trend. The rate parameter decreased when increasing metal concentration. This is consistent with the results presented by Prasanna Kumar et al. [35] using *Ulva fasciata* sp. for zinc sorption. The variation of the rate parameter was significant between 15 and 50 mg L^{-1}, but the parameter tended to stabilize above 50 mg L^{-1} (Table 2). With a sorbent dosage of 0.2 gL^{-1}, the equilibrium was reached after 24 h of contact, and more than 90% of mercury was recovered at the concentration of 15 mg L^{-1}.

The optimization of the process should take into account the objective of the treatment: complete metal recovery (in this case the sorbent dosage should be increased accordingly to metal concentration) or saturation of the sorbent (the mass ratio biomass/metal should be decreased, and the sorption should be operated in successive batches or in column system).

Uptake Kinetics at pH7

Increasing the pH allowed increasing sorption capacity (Figs. 3 and 4). Some complementary experiments have been performed at pH7 using *L. nigrescens*. Sorbent dosage and metal concentrations were varied (Fig. 9). Under the most favorable conditions (i.e., low metal concentration or high sorbent dosage), the equilibrium was reached within 12 h of contact, and the efficiency of the process exceeded 90%. The pseudo-second-order rate equation again fitted experimental data well. Contrary to the sorption capacity that tended to increase with increasing pH, the rate parameter k_2 tended to decrease (Table 3) when compared to the values obtained at pH6 (Table 2).

Influence of the Composition of the Solution on the Sorption of Hg(II)

The composition of the solution is a critical parameter for the efficiency of the sorption process. The presence of salts, the presence of competitor metals, may strongly impact the sorption

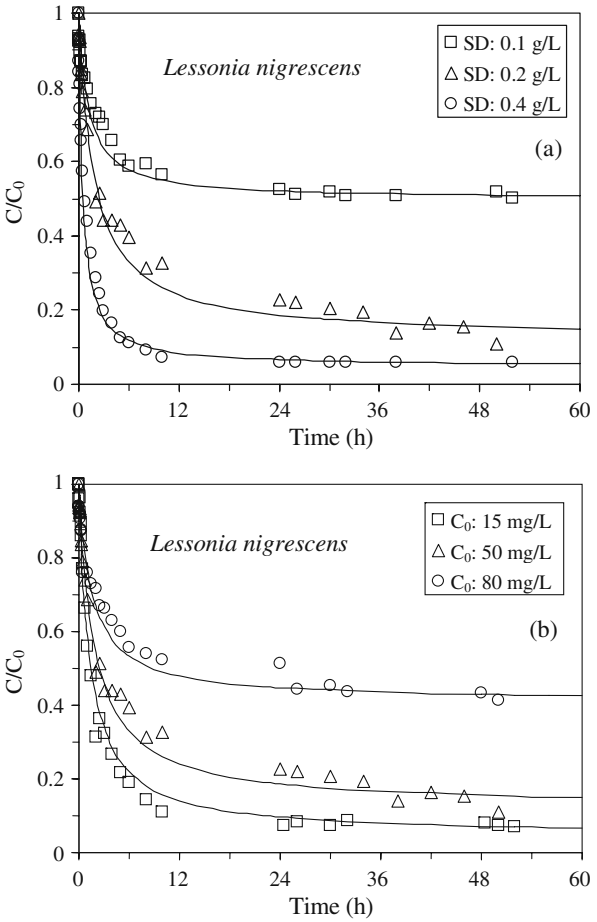

Fig. 9 Hg(II) uptake kinetics using treated biomass of *L. nigrescens*—influence of sorbent dosage (**a**),and metal concentration (**b**) (standard conditions: SD 0.2 gL^{-1}; pH_i7; PS 125–250 μm; *T* 20 °C, *v* 400 rpm)

Table 3 Modeling of uptake kinetics using the pseudo-second-order rate equation for Hg(II) sorption using *L. nigrescens* at pH7 (PS 125–250 μm).

C_0 (mg L^{-1})	SD (g L^{-1})	q_{exp} (mg g^{-1})	q_{eq} (mg g^{-1})	$k_2 \times 10^4$ (g $mg^{-1} min^{-1}$)	R^2
50	0.4	113.4	114.9	3.03	1.000
50	0.2	218.0	214.5	0.42	0.997
50	0.1	229.4	241.3	0.60	0.999
15	0.2	63.4	64.4	1.95	0.999
80	0.2	238.0	239.5	0.45	0.997

process. Figure 10 shows the influence of the addition of increasing concentrations of various salts (i.e., sodium nitrate, sodium chloride, and sodium sulfate) on the efficiency of sorption under given experimental conditions. The addition of sodium nitrate or sodium sulfate in the solution, even at concentrations as high as 0.8 M, did not drastically change the sorption efficiency while a concentration as low as 0.2 M of sodium chloride completely inhibited Hg(II) sorption efficiency (below 5%, compared to 60–62% for the reference experiment) for both *L. nigrescens* and *L. trabeculata* (both sorbents were pretreated). The differential effect of sodium chloride against other sodium salt indicates that this is not the ionic strength

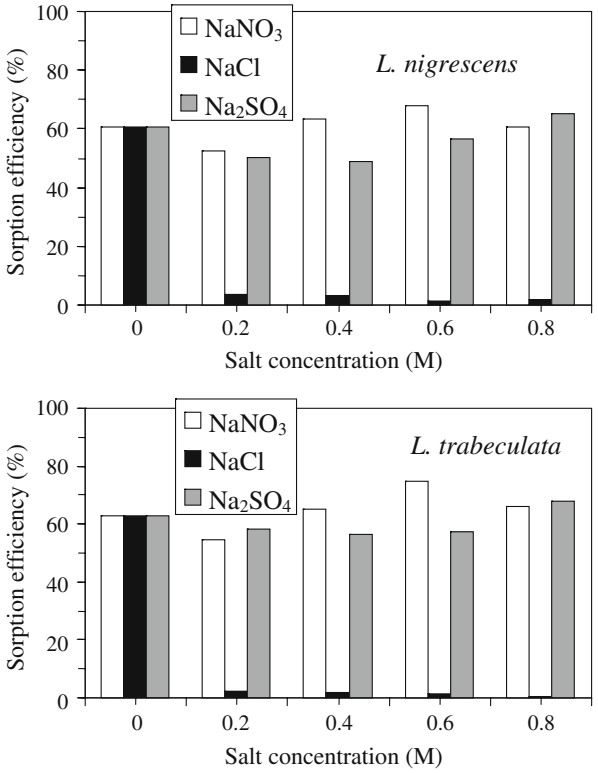

Fig. 10 Influence of the concentration of salts (sodium nitrate, sodium chloride, and sodium sulfate) on Hg (II) sorption efficiency (C_0 50 mg L^{-1}; PS 125–250 μm; SD 0.2 gL^{-1}; agitation speed 200 rpm; pH6, contact time 3 days)

that controls the sorption efficiency (same ionic strength for $NaNO_3$ and NaCl solutions). The explanation of this difference is probably related to the effect of metal speciation. Indeed, mercury does not form stable complexes with sulfate and nitrate while chloro-complexes of mercury are very stable. In the presence of high concentrations of chloride ions, $HgCl_3^-$ and $HgCl_4^{2-}$ species are formed. They predominate over $HgCl_2$ when the concentration of chloride ions exceeds 0.1 M. At a concentration 0.2 M in chloride ions, anionic mercury species represent more than 70% of mercury (86% at 0.4 M, 93% at 0.6 M and up to 95% at 0.8 M, see Fig. A2 of the Electronic Supplementary Material) [36]. At pH6, carboxylic groups of alginate on the surface of the biosorbent are deprotonated and then unable to bind mercury anionic species.

Figure 11 compares the influence of increasing concentrations of $ZnCl_2$, $CdCl_2$, and $NiCl_2$ on the sorption efficiency of Hg(II). For *L. nigrescens*, the effect of the addition of competitor ions was comparable, regardless of the metal. The sorption efficiency progressively decreased with increasing metal concentration. In the case of *L. trabeculata*, the impact of Zn(II) and Ni(II) on Hg(II) sorption is comparable, resulting in a decrease of 50% of the sorption efficiency at equimolar concentration (i.e., 0.25 mM for each Hg(II) and competitor metal). On the opposite hand, Cd(II) had a much weaker competitor effect: At equimolar concentration, the decrease in sorption was limited to 10%. The reduction reached 46% when the concentration of Cd(II) was three times the mercury concentration (to be compared to a 60% reduction for Zn(II) and Ni(II)). The

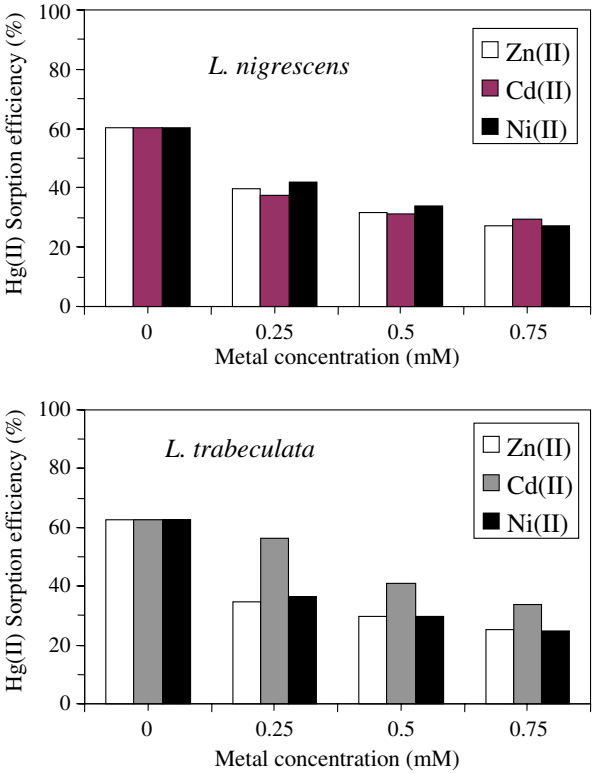

Fig. 11 Influence of the concentration of competitor metal (chloride form) on Hg(II) sorption efficiency (C_0 50 mg L^{-1}; PS 125–250 µm; SD 0.2 gL^{-1}; agitation speed 200 rpm; pH6, contact time 3 days)

decrease in sorption efficiency may be explained by two effects: (a) the addition of supplementary chloride ions that may affect Hg(II) speciation and (b) the competition of these cations for binding on carboxylate groups. Chen et al. [37] used alginate-immobilized *Microcystis aeruginosa* for the sorption of mercury in the presence of Cd (II) and Pb(II): They also pointed out the weak effect of Cd(II) on Hg(II) sorption compared to the impact of Pb(II). These results show that the biosorbents were not selective for Hg(II) sorption under selected conditions.

Mercury Desorption

The best results (with desorption efficiency greater than 90%) were obtained with nitric acid and citric acid and with KI in acidic media. Cycles of sorption/desorption were performed in order to verify the possibility to reuse the sorbent. The solution of KI in acidic media allows maintaining high-desorption yield along sorption/desorption cycles but at the expense of a reduced sorption efficiency. On the opposite hand, 0.05 M citric acid solution maintained high-sorption efficiency along the cycles, but desorption efficiency remained around 60%. Complementary studies are required for optimizing the process; however, it will be probably more interesting considering the biosorbent as a one-use material to be destroyed after being used.

Conclusions

Lessonia spp. (indifferently *L. nigrescens* and *L. trabeculata*) are efficient sorbents for mercury recovery from near neutral solutions. The sorption efficiency and sorption capacities increase with pH. At pH6, sorption capacities as high as 240–270 mg g^{-1} were obtained (i.e., 1.2–1.35 mmol g^{-1}); this is less than the sorption levels reached with specific resins, but this is comparable and even better than many biosorbents commonly cited. The sorption efficiency is strongly controlled by the composition of the solution: The presence of chloride ions affects the speciation of mercury and limits the sorption efficiency. On the other hand, the presence of competitor cations also decreases sorption yield making the biosorbent not selective for Hg(II) in the presence of base metals such as Cd(II), Zn(II), and Ni(II). The sorption process is not controlled by the resistance to intraparticle diffusion, and the uptake kinetics are efficiently described by the pseudo-second-order rate equation. The kinetic coefficient varies in function of experimental parameters such as sorbent dosage, metal concentration, and less with the particle size. SEM-EDAX analysis allows identifying some heterogeneity in the distribution of mercury when adsorbed on the surface of the biomass.

Acknowledgements Authors thank the European Commission for the funding of the project BIOPROAM (Contract no. AML/190901/06/18414/II-0548-FC-FA, in the framework of ALFA program). Authors acknowledge Jean-Marie Taulemesse (Centre des Matériaux de Grande Diffusion at Ecole des Mines d'Alès) for his technical support for SEM-EDAX analysis.

References

1. Patterson, J. (1997). *Aqueous Mercury Treatment*. Washington: U.S.E.P.A.
2. Matlock, M. M., Howerton, B. S., & Atwood, D. A. (2001). *Journal of Hazardous Materials, B84*, 73–82.
3. Kuncoro, E. P., Roussy, J., & Guibal, E. (2005). *Sep. Sci. Technol., 40*, 659–684.

4. Duche, S. N., Pawar, S. D., & Dhadke, P. M. (2002). *Separation Science and Technology, 37*, 2215–2229.
5. Meera, R., Francis, T., & Reddy, M. L. P. (2001). *Hydrometallurgy, 61*, 93–103.
6. Vieira, R. S., Guibal, E., Silva, E. A., & Beppu, M. M. (2007). *Adsorption-Journal of the International Adsorption Society, 13*, 603–611.
7. Atia, A. A., Donia, A. M., & Elwakeel, K. Z. (2005). *Reactive and Functional Polymers, 65*, 267–275.
8. Guibal, E., Gavilan, K. C., Bunio, P., Vincent, T., & Trochimczuk, A. (2007). *Separation Science and Technology, 43*, 2406–2433.
9. Volesky, B., & Holan, Z. R. (1995). *Biotechnology Progress, 11*, 235–250.
10. Zeroual, Y., Moutaouakkil, A., Dzairi, F. Z., Talbi, M., Chung, P. U., Lee, K., et al. (2003). *Bioresource Technology, 90*, 349–351.
11. Vilar, V. J. P., Botelho, C. M. S., & Boaventura, R. A. R. (2008). *Biochemical Engineering Journal, 38*, 319–325.
12. Svecova, L., Spanelova, M., Kubal, M., & Guibal, E. (2006). *Separation and Purification Technology, 52*, 142–153.
13. Vijayaraghavan, K., & Yun, Y.-Y. (2008). *Biotechnology Advances, 26*, 266–291.
14. de França, F., Padilha, F., & da Costa, A. (2006). *Applied Biochemistry and Biotechnology, 128*, 23–32.
15. Michalak, I. & Chojnacka, K. (2009). Applied Biochemistry and Biotechnology. doi:10.1007/s12010-12009-18635-12017.
16. Picardo, M., de Melo Ferreira, A., & da Costa, A. (2006). *Applied Biochemistry and Biotechnology, 134*, 193–206.
17. Romera, E., González, F., Ballester, A., Blázquez, M. L., & Muñoz, J. A. (2007). *Bioresource Technology, 98*, 3344–3353.
18. Tajes-Martinez, P., Beceiro-Gonzalez, E., Muniategui-Lorenzo, S., & Prada-Rodriguez, D. (2006). *Talanta, 68*, 1489–1496.
19. Fourest, E., & Volesky, B. (1997). *Applied Biochemistry and Biotechnology, 67*, 215–226.
20. Dubois, M. A., Dozol, J. F., & Massiani, C. (1995). *Journal of Analytical and Applied Pyrolysis, 31*, 129–140.
21. Reategui, M., Maldonado, H., Ly, M., & Guibal, E. (2009). *Advances in Materials Research, 71–73*, 585–588.
22. Decarvalho, R. P., Chong, K. H., & Volesky, B. (1994). *Biotechnological Letters, 16*, 875–880.
23. Matheickal, J. T., Yu, Q., & Woodburn, G. M. (1999). *Water Research, 33*, 335–342.
24. Ho, Y. S. (2006). *Water Research, 40*, 119–125.
25. Liu, Y., & Liu, Y.-Y. (2007). *Separation and Purification Technology, 61*, 229–242.
26. Mata, Y. N., Blázquez, M. L., Ballester, A., González, F., & Muñoz, J. A. (2008). *Journal of Hazardous Materials, 158*, 316–323.
27. Davis, T. A., Volesky, B., & Mucci, A. (2003). *Water Research, 37*, 4311–4330.
28. Malik, D. J., Streat, M., & Greig, J. (1999). *Institution of Chemical Engineers Translations, 77*, 227–233.
29. Hansen, H. K., Ribeiro, A., & Mateus, E. (2006). *Minerals Engineering, 19*, 486–490.
30. Ghodbane, I., & Hamdaoui, O. (2008). *Journal of Hazardous Materials, 160*, 301–309.
31. Kaçar, Y., Arpa, C., Tan, S., Denizli, A., Genç, O., & Arica, Y. (2002). *Process Biochemistry, 37*, 601–610.
32. Bayramoglu, G., Tuzun, I., Celik, G., Yilmaz, M., & Arica, M. Y. (2006). *International Journal of Mineral Processing, 81*, 35–43.
33. Lloyd-Jones, P. J., Rangel-Mendez, J. R., & Streat, M. (2004). *Institution of Chemical Engineers Translations, 82B*, 301–311.
34. Pavasant, P., Apiratikul, R., Sungkhum, V., Suthiparinyanont, P., Wattanachira, S., & Marhaba, T. F. (2006). *Bioresource Technology, 97*, 2321–2329.
35. Prasanna Kumar, Y., King, P., & Prasad, V. S. R. K. (2007). *Chemical Engineering Journal, 129*, 161–166.
36. Make Equilibrium Diagrams Using Sophisticated Algorithms (MEDUSA) (2002) v. 3.1. http://www.kemi.kth.se/medusa. Accessed 7 February 2007.
37. Chen, J. Z., Tao, X. C., Xu, J., Zhang, T., & Liu, Z. L. (2005). *Process Biochemistry, 40*, 3675–3679.